Functional Materials 11, No.1 (2004)

Analysis of design characteristics of the prototype ionization chamber and beam loss monitor for proton accelerator facilities in Korea

Jae Cheon Kim, Jong Kyung Kim, Yong Kyun Kim, Se Hwan Park**

Hanyang University, Haengdang-dong, Seongdong-gu, Seoul, Korea
*Korea Atomic Energy Research Institute,
Deokjin-dong, Yuseong-gu, Daejeon, Korea

To investigate the design characteristics of the newly designed and fabricated prototype ionization chamber, which was made by cooperation with KAERI (Korea Atomic Energy Research Institute), the absorbed dose of inner gas was calculated and measured. The variations of the electric current of the above chambers were investigated at incident energies between 40 keV and 1 MeV using Monte Carlo codes such as EGSnrc (DOSRZnrc) and MCNP4C. Some calculations and measurements were performed to investigate their current variations as the incident angle of gamma-rays was changed from 0° to 90° and as the length of collecting electrode was changed from 10 mm to 20 mm. Some calculations were carried out to improve the collection efficiency of the ionization chamber for the beam loss monitor through replacement of wall (collecting electrode) material and inner gas. The influence due to improvement features of EGSnrc and MCNP4C was investigated through calculations of the depth dose distributions for broad beams of monoenergetic electrons with energies of 25 keV to 4 MeV, incident normally on water.

Для исследования характеристик конструкции вновь разработанного и изготовленного прототипа ионизационной камеры, выполненного в сотрудничестве с KAERI (Корейским Исследовательским Институтом Атомной Энергии), рассчитывались и измерялись дозы радиации, поглощенной внутренней газовой средой камеры. Изменения электрического тока в вышеупомянутых камерах исследовались при значениях энергии падающего излучения от 40 кэВ до 1 МэВ с применением кодов Монте-Карло, например, EGSnrc (DOSRZnrc) и MCNP4C. Проведены некоторые расчеты и измерения для исследования изменений тока при изменении угла падения гамма-лучей от 0° до 90° и изменении длины коллекторного электрода от 10 до 20 мм. Выполнены некоторые расчеты с целью повышения показателя эффективности сбора ионизационной камеры для монитора потерь пучка путем замены материала стенки (коллекторного электрода) и газовой среды. Исследовано влияние усовершенствования EGSnrc и MCNP4C путем расчетов распределения дозы по глубине для широких пучков моноэнергетических электронов с энергиями от 25 кэВ до 4 МэВ, падающих нормально на поверхность воды.

Much attention has been paid to the radiation detector technology in Korea. In recent years, some investigations also have been performed to develop the technologies in relation to the radiation detector such as design, fabrication, analysis and et al.

The air-filled ionization chamber is required to satisfy some standards for measuring the absorbed dose of inner gas. The newly designed ionization chamber is necessary to be reviewed whether the electric current linearly increases with incident radiation energy or not and whether it is dependent on the incident source angle or not. The above two were intensively analyzed for newly designed prototype ionization cham-

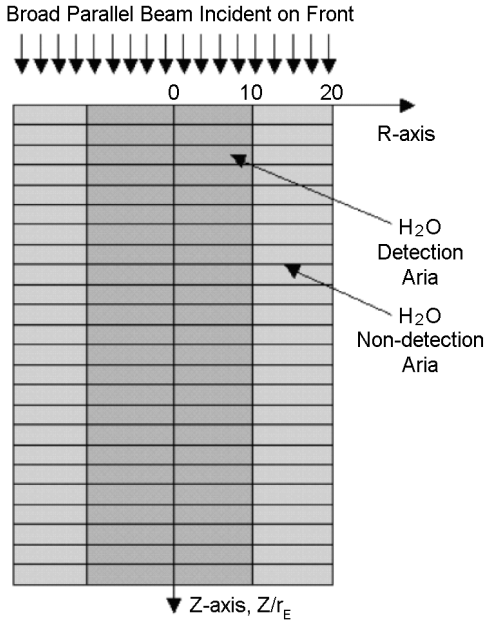

Fig. 1. Broad parallel beams of monoenergetic electrons incident normally on the surface of the semi-infinite water.

bers in this study. The absorbed dose of inner gas of the ionization chambers, that can be directly transformed to the electric current, was calculated to investigate the design characteristics and to find out more efficient and optimized chamber using EGSnrc [1], and MCNP4C [2]. In this work, DOSRZnrc [3], that is the one among NRC user codes, was used for all the calculations using EGSnrc.

An 100 MeV, 20 mA proton linear accelerator is being constructed in Korea. An accelerator facility with such a high intensity beam needs the beam loss monitoring system for the primary diagnostic tool for tuning and preventing excess activation and equipment damage. Ionization chambers have been mainly used as the beam loss monitor (BLM) for an accelerator facility because of their stability, sample uniformity, flat response over a wide voltage range, and sensitivity. But an ionization chamber for the BLM has concerns about slow ion collection times and low collection efficiency at high loss rates.

The Monte Carlo codes such as EGSnrc and MCNP4C are widely used for photon and electron transport. In 2000, EGSnrc and MCNP4C included many improvement features in electron transport algorithms, electron library and et al. Some comparisons between above Monte Carlo codes were performed to investigate the influence due to improvement features.

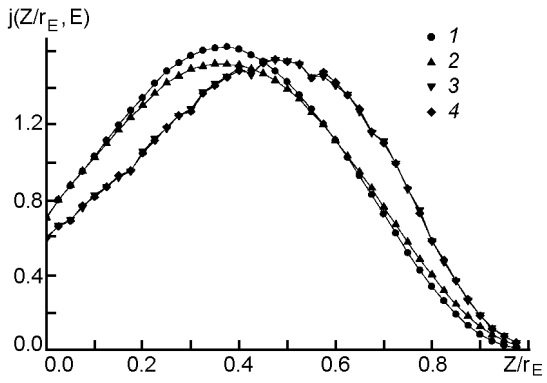

Fig. 2. Comparison of the depth doses in semi-infinite water calculated for a broad parallel beam of 25 keV electrons using EGSnrc, EGS4, MCNP4C, and MCNP4B.

1 — EGS4; *2* — EGSnrc; *3* — MCNP4C; *4* — MCNP4B.

EGSnrc (NRCC) and MCNP4C (Los Alamos) were upgraded from EGS4 (SLAC) and from MCNP4B in 2000, respectively. EGSnrc adopts a new multiple scattering theory, new elastic electron scattering cross sections (involving relativistic and spin effects), and a new electron-step algorithm, the PRESTA-II algorithm. MCNP4C was also improved by replacement of the electron library and electron physics enhancements such as density effect calculation for stopping power, bremsstrahlung production, and et al.

It was assumed the electron beams with energies of 25 keV to 4 MeV entered a plane water surface at normal incidence to calculate the absorbed dose at a given depth of water in Fig. 1. The water was equally divided into 48 planar slices, parallel to the surface. Slice thickness was $0.025\,r_E$ (mean range of electron). Using EGSnrc, EGS4, MCNP4C, and MCNP4B, the absorbed dose in each water slice was calculated for each electron beams.

It is known that double backscattering, from water to air to water, in principle would have increased the dose near the surface. However, double backscattering was ignored in this work since the electrons were assumed to come from vacuum rather than from air.

In DOSRZnrc and MCNP4C, *dose and stoppers (IFULL)* and F8* were used for tally option to calculate the absorbed dose at a given depth, respectively. In all simulations, photon and electron transport energy cut-off were 1 keV. The dimensionless depth dose was introduced for convenience

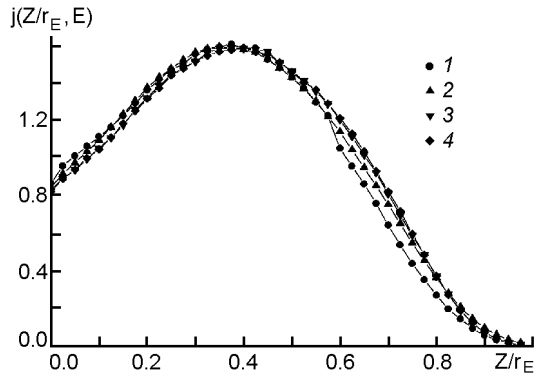

Fig. 3. Comparison of the depth doses in semi-infinite water calculated for a broad parallel beam of 1MeV electrons using EGS4 (*1*), EGSnrc (*2*), MCNP4C (*3*), and MCNP4B (*4*).

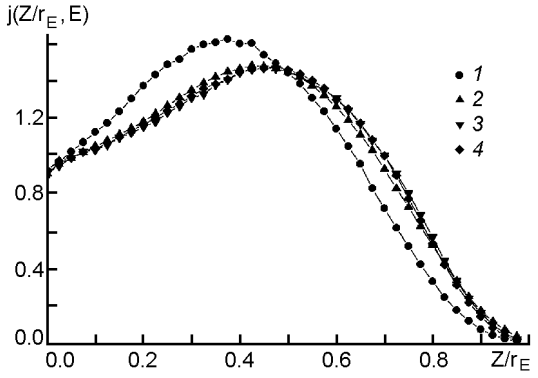

Fig. 4. Comparison of the depth doses in semi-infinite water calculated for a broad parallel beam of 4 MeV electrons using EGS4 (*1*), EGSnrc (*2*), MCNP4C (*3*), and MCNP4B (*4*).

and can be easily obtained using mean range and incident electron energy: as follows,

$$j(Z/r_E,E) = J(Z/r_E,E) \cdot r_E/E.$$

Fig. 2 to Fig. 4 show the dimensionless depth dose distribution for the electron beams with energies of 25 keV, 1 MeV, and 4 MeV. Through simulations, MCNP4C and MCNP4B gave a higher dose compared to EGSnrc and EGS4 inner R_{50} (at shallow position from source) whereas the former gave a lower dose compared to the latter outer R_{50} in the low-energy (<1 MeV) region as can be shown in Fig. 2. Fig. 4 shows EGS4 also gives a higher dose compared to the others inner R_{50} in high-energy (>1 MeV) region.

As can be shown in Fig. 5, the total absorbed dose in semi-infinite water calculated by MCNP4C/MCNP4B is a little higher than that calculated by EGSnrc/EGS4 in all energy region. The deviation of the total absorbed dose between EGSnrc and EGS4 is about 0.58 % (Root Mean Square). The difference between MCNP4B and MCNP4C is smaller than that between EGSnrc and EGS4, within 0.043 %.

These differences and tendency partially attributed to the different multiple scattering theories and Monte Carlo models for electron transport adopted in these codes. MCNP4C has a small change such as electron library and some transport options based on a Class I Monte Carlo Model whereas EGSnrc adopted new multiple scattering theory and electron step algorithm such as PRESTA-II. It is found that there are some more changes in EGSnrc compared to MCNP4C through simulations.

Three types of the ionization chambers

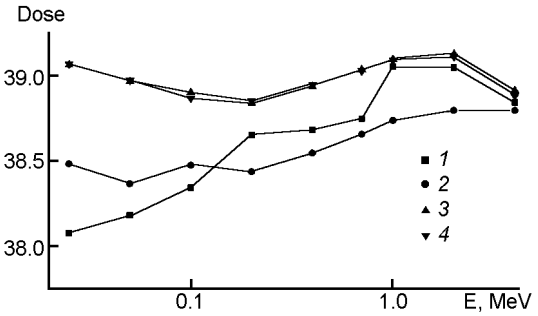

Fig. 5. Comparison of the total absorbed doses in semi-infinite water calculated for broad parallel beams of electrons with energies of 25 keV to 4 MeV electrons using EGSnrc (*1*), EGS4 (*2*), MCNP4C (*3*), and MCNP4B (*4*).

were designed and fabricated as shown in Fig. 6. These are based on the Exradin A12 Farmer type ionization chamber. The Exradin A12 chamber is a farmer-type thimble chamber and is made of air-equivalent plastic C552. The chamber is particularly suited for calibration of therapy beams in terms of absorbed dose in water in accordance with established protocols such as that published by the American Association of Physicists in Medicine.

KAERI-F is the ionization chamber with flat-type window. KAERI-SR and KAERI-LR have a round-type window. The former is short and the latter is long. The ionization chambers with round-type window (KAERI-SR and KAERI-LR) were introduced to improve the angular dependence in

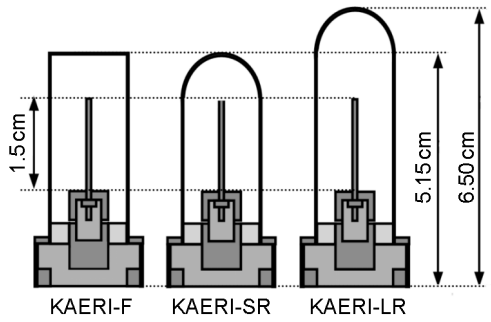

Fig. 6. The cross-sectional view of the ionization chamber with various window type designed and simulated.

this work. All of the chambers have the cavity diameter of 12 mm and the cavity length of about 28 mm. The wall thickness is 1 mm. The length and the diameter of the collecting electrode were 15 mm and 1 mm, respectively.

Most part of the ionization chamber such as wall, window, and collecting electrode consist of PVDF (Polyvinylidene fluoride) known for air-equivalent plastic. Teflon is used as insulation material of guard region between electrode and wall. The detector was filled with the typical air gas. Fig. 7 shows the picture of the ionization chamber with flat-type window.

The present investigation focused on the angular dependence, the energy linearity of the ionization chamber, and the influence on length variations of collecting electrode. ^{241}Am and ^{137}Cs were used as the source for simulation and experiment. The distance to source from the rotation point of the ionization chamber is 7 cm. The rotation point is 1.77 cm under the surface of window of flat-type ionization chamber.

The *dose and stoppers* (IFULL) was used for tally option of DOSRZnrc. The maximum fractional energy loss per step (ESTEPE) was 0.25 and photon/electron energy cut-off was 1 keV, respectively. For MCNP4C, F8* tally, which estimates the energy deposited in the cell, was used for dose calculation. The energy cut-off for photon was 1 keV, which was the same as in DOSRZnrc.

Monte Carlo codes cannot directly simulate the electric current. But the absorbed dose of inner gas of ionization chamber can be easily calculated. In this context, this study introduced a conversion factor of *W*-value, which was defined as the average energy needed for producing one ion-pair as the radiation goes through any specific gas.

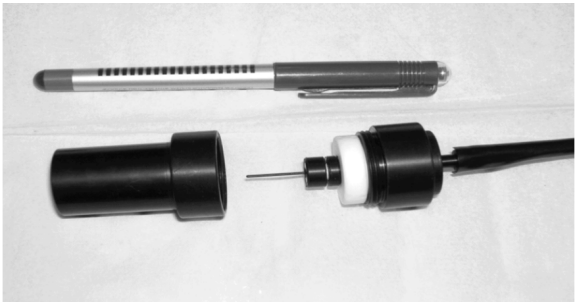

Fig. 7. The flat-type ionization chamber fabricated.

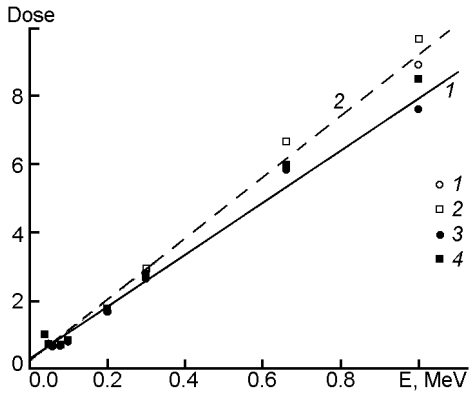

Fig. 8. The current variations of the ionization chamber by changing incident gamma-ray energy from 40 keV to 1 MeV calculated by EGSnrc, MCNP4C. *1* — flat (MCNP4C); *2* — short round (MCNP4C); *3* — flat EGSnrc; *4* — short round (EGSnrc).

Finally, the electric current of the ionization chamber can be easily obtained by the calculated absorbed dose and *W*-value, as follows:

$$\text{Electric current} = \frac{\text{Absorbed dose}}{W - \text{value}}.$$

The electric current of the designed ionization chamber was computed to review the energy linearity with the incident gamma-ray energy. The gamma-ray energy changed from 40 keV to 1 MeV, and current variations are shown in Fig. 8. The results of simulation show that the electric current of KAERI-F and KAERI-SR linearly increases with the incident gamma-ray energy. The solid and the dotted line linearly fit the results of the MCNP4C and EGSnrc for the flat-type window, respectively.

The electric current calculated by MCNP4C tends to be greater than that by DOSRZnrc. The current of MCNP4C was greater than that of EGSnrc in KAERI-F, about 7.2 % and in KAERI-SR, about 31.7 %. Most statistical error was within

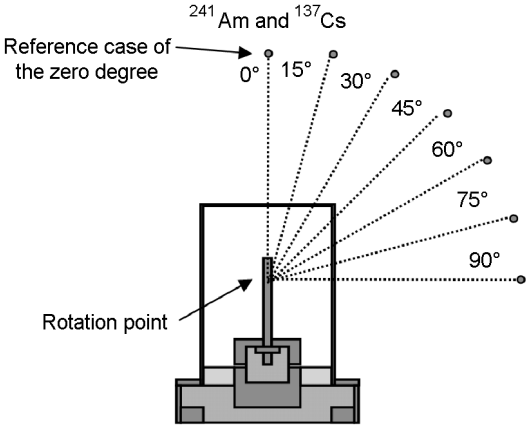

Fig. 9. The variation of the source angle incident on the ionization chamber.

5 %. However, the error reached 15 % in the calculation of the electric current of the ionization chamber with round-type window. It is attributed to the fact that the inner gas was modeled by the air-filled and very small cell in DOSRZnrc calculation for the ionization chamber with round-type window.

For the analysis of angular dependence of the ionization chamber, the source angle was changed from zero degree to 90 degree. The source in the reference case was located vertically above the window of the ionization chamber in Fig. 9. The electric current was normalized to the value in the reference case of zero degree. Therefore, the normalized electric current is obtained by

$$\text{Normalized electric current} = \frac{\text{Current at a given angle}}{\text{Current at the reference angle}}$$

When ^{241}Am was used for an isotropic point photon source and the type of an ionization chamber was KAERI-F, the maximum current difference calculated by DOSRZnrc and MCNP4C was 7 % and 10 %, respectively. Experimental measurements were 6.5 %. In case of KAERI-SR, the maximum current difference calculated by MCNP4C was 3 % and measurements was 2.6 %. In case of KAERI-LR, the former was 22 % and the latter was 18 %, respectively.

As a whole, the current variation by changing source angle tends to increase with the incident source energy as can be shown in Fig. 11. When ^{137}Cs was used and the type was KAERI-F, the maximum current difference obtained by DOSRZnrc, MCNP4C, and measurements was 12 %, 9 %, and 7.4 %, respectively. The statistical error was similar to that by the calculation for energy linearity of the ionization chamber. In case of KAERI-SR, the maximum current difference calculated by MCNP4C was 2 % and measurements was 5.9 %. In case of KAERI-LR, the maximum difference obtained by MCNP4C was 28 %.

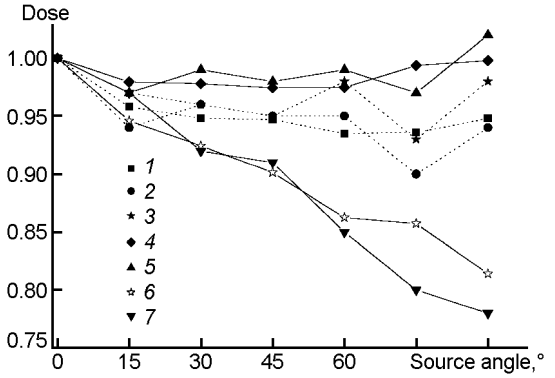

Fig. 10. The comparison of the doses of KAERI-F, KAERI-SR, and KAERI-LR produced by ^{241}Am. *1* — flat (Exp); *2* — flat (MCNP4C); *3* —flat (EGSnrc); *4* — short round (Exp); *5* — short round (MCNP4C); *6* — long round (Exp); *7* — long round (MCNP4C).

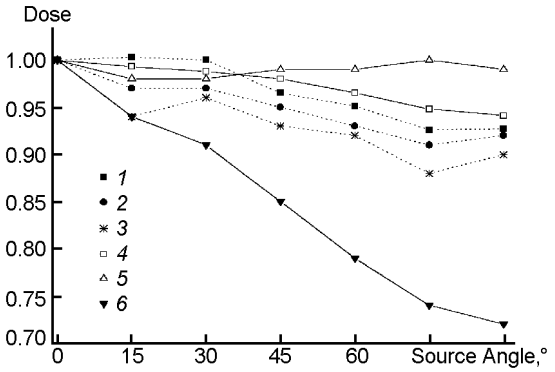

Fig. 11. The comparison of the doses of KAERI-F, KAERI-SR, and KAERI-LR produced by ^{137}Cs. *1* — flat (Exp); *2* — flat (MCNP4C); *3* — flat (EGSnrc); *4* — short round (Exp); *5* — short round (MCNP4C); *6* — long round (MCNP4C).

Through simulations and measurements, it is found that KAERI-SR with short and round-type window is less dependent on incident source angle compared to the others. Fig. 12 shows the experiment to obtain the measurements in relation to the angular dependence of KAERI-SR. The experiments of KAERI-F and KAERI-LR were also implemented in the same condition.

Through DOSRZnrc calculations, the influence on length variations of collecting electrode was investigated on the KAERI-F.

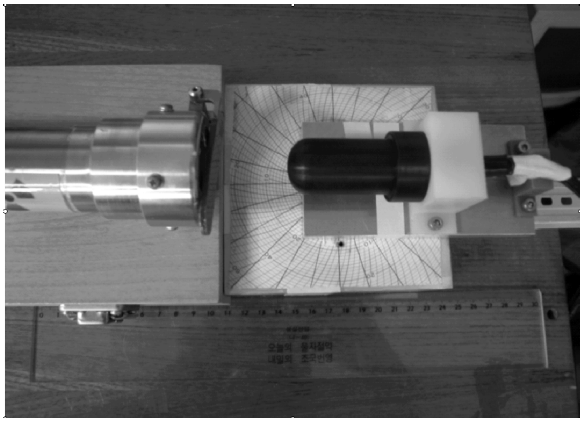

Fig. 12. The experiment for analysis of angular dependence using short round-type ionization chamber.

The designed original length of collecting electrode of KAERI-F is 15 mm. The length was changed from 10 mm to 20 mm by 2.5 mm. In this work, two methods were used to estimate the efficiency of the ionization chamber. First, the total volume of air gas producing current was fixed and the inner wall diameter was changed. Second, the volume was changed and the inner diameter was fixed with the length variations.

As shown in Fig. 13, the maximum current was at 12.5 mm. But the difference of the current was calculated within ±1 %, which was found to be negligible.

A prototype ion chamber for the BLM was designed of two concentric cylinders filled with air as shown in Fig. 14. The cylinder was 210 mm long and made of 2 mm thick aluminum. The diameter of outer electrode was 38 mm. The inner electrode was hollow and filled with air inside. Guard electrode was made of copper, and it was placed in the middle of the inner electrode and the outer electrode. Teflon insulators were placed between electrodes. The ion chamber was housed inside the 2 mm thick aluminum cylinder [4].

In general, an ion chambers for the BLM are needed to overcome concerns about slow ion collection times and low collection efficiency at high loss rates although there are many advantageous features. Both are considerably related to the electrical parameters such as applying voltage, electrode gap, ionization charge density, and so on. The collection efficiency f of an ion chamber at a given bias voltage V can be defined as the ratio of the measured current to the ideal saturation current. The equations for describing f have been known since Thomson described them in 1899 [5]: as follows,

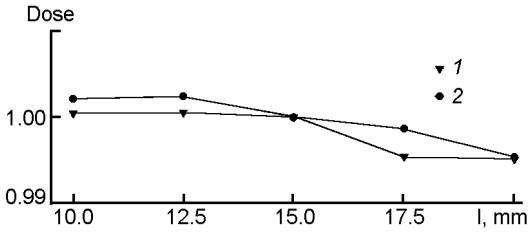

Fig. 13. The variation of the electric current according to changing the length of collecting electrode. *1* — Gas Volume Fixed; *2* — Wall Fixed.

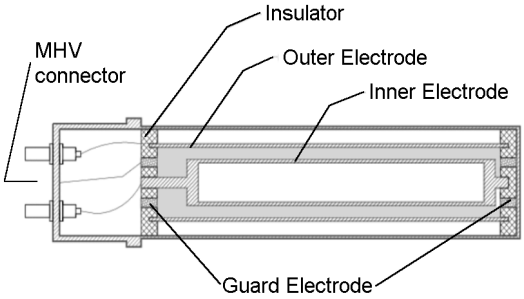

Fig. 14. Prototype ion chamber for beam loss monitor.

$$f = \frac{1}{1+\xi^2}, \quad \xi^2 = \left(\frac{\alpha}{6ek_1k_2}\right)\left(\frac{d^4}{V^2}\right)\left(\frac{q}{vol}\right),$$

$$\begin{cases} e\text{:electron charge} \\ \alpha\text{:first Townsend recombination coeff.} \\ k_i\text{:electron mobility} \\ k_2\text{:ion mobility} \\ q\text{:ionization charge density} \end{cases}$$

Instead of changing electrical parameters, replacement of wall (outer electrode) material or inner gas of the BLM was tried to improve the collection efficiency of ionization chamber. The absorbed dose of inner gas was calculated to obtain the ionization charge density q of a given wall material. The energy deposited in the gas volume of an ionization chamber is proportional to the ionization charge density. And the former is proportional to $1/q^2$.

The relative collection efficiency is calculated from the absorbed dose of inner gas. The collection efficiency at incident photon energy was normalized to that at 60 keV. Therefore, the relative collection efficiency is obtained by

$$\text{Relative Collection Efficiency} = \frac{(D^k_{60keV})^2}{(D^k_c)^2}.$$

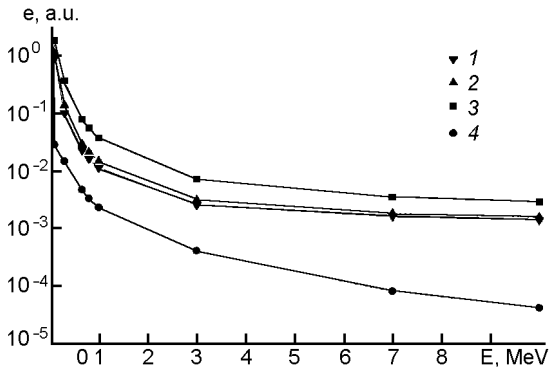

Fig. 15. The variation of relative collection efficiency of the ion chamber for the beam loss monitor by replacement of wall material. *1* — PMMA; *2* — PVDF; *3* — Aluminum; *4* — Copper.

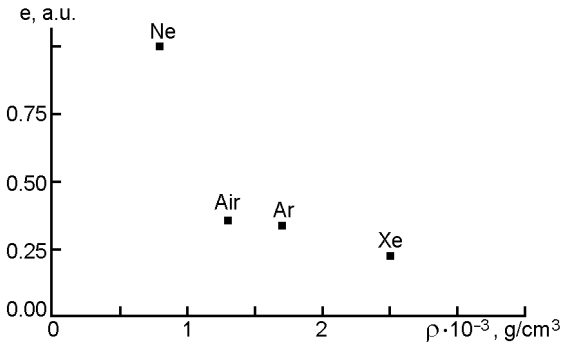

Fig. 16. The absorbed dose variation of the ion chamber for the beam loss monitor by replacement of inner gas.

Here, k is the wall material used, e is the photon source energy, and D is the absorbed energy of inner gas. PMMA, PVDF, aluminum, and copper were used for wall material of BLM. To investigate the influence of replacement of inner gas used for BLM, Ne, air, Ar, and Xe were considered, respectively. Table shows the density of wall materials and inner gases.

Using DOSRZnrc, the absorbed doses for an isotropic photon source with energies of 60 keV to 10 MeV were calculated and were transformed to the value of the relative collection efficiency. In the DOSRZnrc results, it was found that the wall material made by aluminum was more efficient than the others as shown in Fig. 15.

To investigate the influence due to replacement of inner gas, the absorbed dose of the BLM with PVDF outer electrode wall was calculated when the incident photon energy was 1 MeV. The collection efficiency of a given inner gas was also normalized to that of Ne-gas. Fig. 16 shows that the collection efficiency decreases as the density of inner gas and Z number increases.

In conclusions, in this study, three types of the ionization chamber were designed and fabricated to investigate the design characteristics. All the designed ionization chambers showed the electric current was linearly increased with the incident gamma-ray energy. KAERI-SR was less dependent on the source angle than the others. Its maximum difference was 3.0 % in case of ^{241}Am, 5.9 % in case of ^{137}Cs. It was found that the angular dependence of the ionization chamber was reduced as the length of the chamber was decreased and a round-type window was adopted. The difference of the electric current due to the length variation of collecting electrode was negligible, within 1 %.

To improve the collection efficiency of the ionization chamber for the BLM, we replaced either the wall materials or inner gas of the BLM. It was shown that the use of aluminum as the wall material could obtain a higher collection efficiency than the others. In case of replacing the inner gas, the collection efficiency was increased as the inner gas density and its Z number were decreased.

Additionally, the influence due to improvement features of EGSnrc and MCNP4C was investigated through calculations of the depth dose distributions at the water. MCNP4C and MCNP4B tends to give a higher dose compared to EGSnrc and EGS4 inner R50 whereas the former give a lower dose compared to the latter outer R_{50} in the low energy (<1 MeV) region. The total absorbed dose calculated by MCNP4C and MCNP4B has a tendency to be a little higher than that calculated by EGSnrc and EGS4 at incident energies between 25 keV and 4 MeV.

Acknowledgement. This work has been supported financially by iTRS (innovative Technology Center for Radiation Safety) and KAERI (Korea Atomic Energy Research Institute).

Table. The density of wall material and inner gas used for beam loss monitor

Gas	Density (g/cm^3)	Wall Material	Density (g/cm^3)
Ne	0.0008	PMMA	1.1900
Air	0.0013	PVDF	1.7600
Ar	0.0017	Aluminum	2.7020
Xe	0.0025	Copper	8.9333

References

1. I.Kawrakow, D.W.O.Rogers, PIRS-701 National Research Council of Canada (2001).
2. J.F.Briesmeister, Report LA-13709-M.
3. D.W.O.Rogers, I.Kawrakow, J.P.Seuntjens, B.R.B.Walters, NRCC Report PIRS-702 (Rev. A), National Research Council of Canada (2001).
4. Se Hwan Park, Yong Kyun Kim, Ki Un Youm et al., ISORD-2 (2003).
5. R.L.Witkover, D.Gassner, SNS-Report (2002).

Аналіз характеристик конструкції прототипу іонізаційної камери та монітора втрат пучка для прискорювачів протонів у Кореї

Чжа Чонг Кім, Чжон Кунг Кім, Йонг Кун Кім, Се Хван Пак

Для дослідження характеристик конструкції новорозробленого та виготовленого прототипу іонізаційної камери, виконаного спільно з KAERI (Корейським Дослідним Інститутом Атомної Енергії), розраховувалися та вимірювалися дози радіації, поглиненої внутрішнім газовим середовищем камери. Зміни електричного струму у вищезгаданих камерах досліджено при значеннях енергії падаючого проміння від 40 кеВ до 1 МеВ з застосуванням кодів Монте-Карло, наприклад, EGSnrc (DOSRZnrc) та MCNP4C. Виконано деякі розрахунки та вимірювання для дослідження змін струму при зміні кута падіння гамма-променів від 0° до 90° і зміні довжини колекторного електрода від 10 до 20 мм. Виконано деякі розрахунки з метою підвищення показника ефективності збору іонізаційної камери для монітора втрат пучка шляхом заміни матеріалу стінки (колекторного електрода) та газового середовища. Досліджено вплив удосконалення EGSnrc та MCNP4C шляхом розрахунків розподілу дози за глибиною для широких пучків моноенергетичних електронів з енергіями від 25 кеВ до 4 МеВ, що падають нормально на поверхню води.